ISTITUTO NAZIONALE DI FISICA NUCLEARE
Sezione di Trieste

INFN/TC-02/09
10 aprile 2002

Irradiation tests of the ALICE Silicon Drift Detector at the LINAC of the "Elettra" Synchrotron in Trieste.

Claudio Piemonte[1], Alexander Rashevsky[2], Alessandro Roncastri[1]
[1)] *Università di Trieste, Dipartimento di Fisica, Via A. Valerio 2, I-34127 Trieste, Italy*
[2)] *INFN, Sezione di Trieste, Via A. Valerio 2, I-34127 Trieste, Italy*

Abstract

Three ALICE-D2 Silicon Drift Detectors were irradiated with $1GeV$ electrons at the LINAC of the "Elettra" Synchrotron in Trieste. The aim of this test was to verify the radiation hardness of the device under an electron fluence equivalent to the particle fluence of ten years of ALICE operation. The anode current, the voltage distribution on the integrated divider and the operation of the MOS injectors were tested. The note reports the results of these tests.

Published by **SIS-Pubblicazioni**
Laboratori Nazionali di Frascati

1 Introduction.

Silicon Drift Detectors will equip the third and fourth layer of the Inner Tracking System (ITS) of the ALICE experiment at CERN [1]. The final version of the detector is called ALICE-D2, and it is the result of an intensive R&D phase [2–5]. Basically, the device is composed by the structures depicted in figure 1. It has two drift regions each formed by

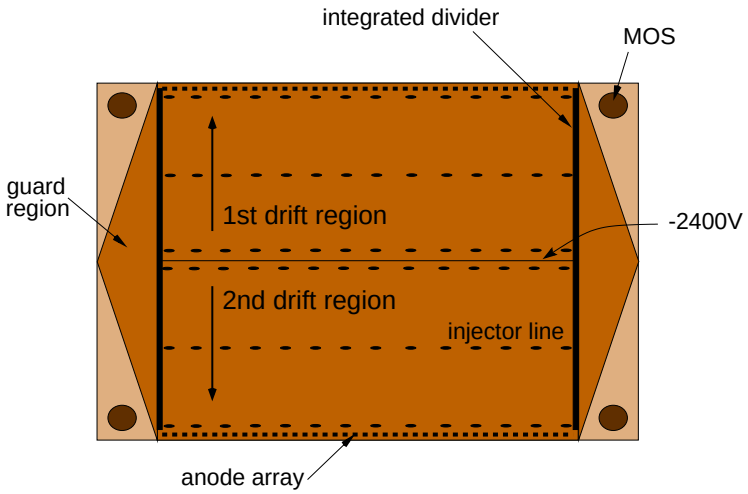

Figure 1: ALICE-D2 detector.

291 cathodes per side with a pitch of $120\,\mu m$. Both regions end with a collection zone which houses an array of 256 anodes for a total length of about $75\,mm$. Three lines of point-like MOS injectors per half-detector allow the monitoring of the drift velocity. At the flanks of the sensitive area there are two triangular guard structures which scale the high negative potentials of the drift cathodes to the ground ring. Between the sensitive region and the two guard regions an integrated divider biases the whole detector. The device is completed, giving it a rectangular shape, by four non-sensitive triangles. Each of these regions contains a MOS capacitor.

One of the steps towards the mass production of the detector is the evaluation of its radiation hardness. In general, a silicon device undergoes to two types of damage due to the impinging radiation: bulk damage [6] and surface damage [7]. The first arises from the displacement of silicon atoms from their lattice sites, creating energy levels within the band gap. Depending on the position of these levels, the macroscopic result is either an additional leakage current or a variation of the effective bulk doping.

The surface damage is related to the holes created by ionization in the silicon dioxide. Either these holes can be captured in long-lived traps near the $Si - SiO_2$ interface increasing the effective positive fixed oxide charge density, or they may create interfacial states increasing the surface component of the leakage current. These last phenomena are

strongly dependent on the bias conditions and on the manufacturing processes.
The main concern for the ALICE SDD is the growth of the leakage current collected by the anodes. In particular the read-out electronics scheme puts a limit of $200nA$ per anode. This requirement poses a severe restriction on the evolution of both the dark current and the magnitude of possible defects generating high current collected by the anodes [9].
On the other side, the hole component of the leakage current is collected by the drift cathodes and enters the integrated divider, affecting the linearity of the potential distribution on the cathodes themselves [9]. This means that the linearity is gradually altered as the particle fluence increases, corrupting in a systematic way the reconstruction of the impact point along the drift direction. This error should be corrected constantly during the lifetime of the experiment.
A structure strongly dependent on the surface conditions is the MOS injector. Indeed, the amplitude of the injector signal at the anodes depends on the number of electrons attracted by the positive fixed oxide charge. Practically, the radiation should not deteriorate the behaviour of this component since it leads to an increase of the positive oxide charge and consequently a growth of the number of electrons trapped beneath the MOS metal.

2 Electron fluence evaluation

The radiation environment of the ALICE experiment is much less critical than the other LHC experiments. The first layer of the silicon drift detectors (third layer of the ITS) has to withstand a total ionizing dose of $13krad$ plus a neutron fluence of $3.5 \times 10^{11}cm^{-2}$ in ten years of operation. Considering also the possibility of a failure during the beam injection [8] the total ionizing dose becomes $14krad$. Simulations of the particle multiplicities evidence that the main contribution to the ionizing dose is given by charged pions. Hence, since the irradiation tests are carried out using $1GeV$ electrons, special care should be taken in order to reproduce the ALICE radiation environment.
Considering the surface damage, in order to create an ALICE-like ionizing energy loss in the silicon dioxide, it is sufficient to reproduce the ALICE total ionizing dose in silicon, i.e. $14krad$. Since the ionizing energy loss of $1GeV$-electrons in silicon is $2.1\,MeVcm^2/g$ the corresponding electron fluence for a $300\mu m$-thick detector is about $5 \times 10^{11}e^-/cm^2$.

As far as the bulk damage is concerned, the fluence evaluation is more complicated. Indeed, the probability to displace an atom from its lattice site depends on the type and energy of the radiation. In order to calculate the electron fluence needed to reproduce the bulk damage due to both the charged pions and neutrons we used the NIEL hypothesis [10]. This hypothesis is based on numerous observations that in silicon the bulk damage

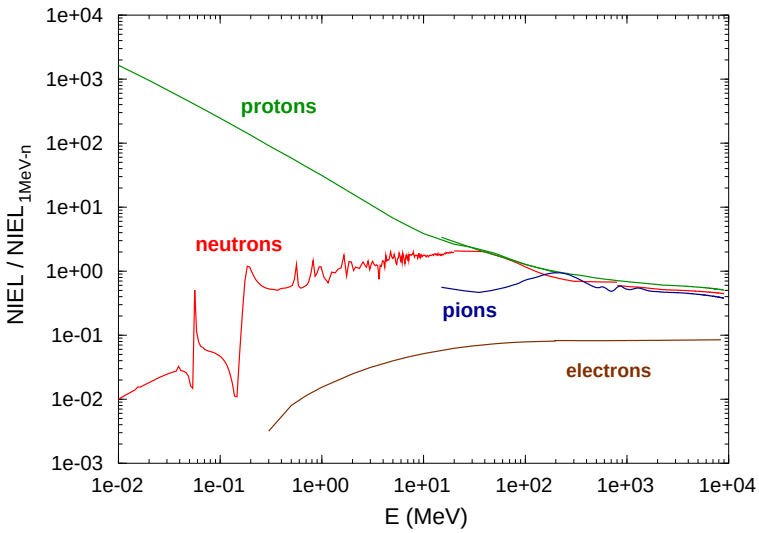

Figure 2: NIEL normalised to $1MeV$-neutron in Silicon for different particles [6].

due to energetic particles is proportional to the non-ionizing energy loss (NIEL). Figure 2 shows the non-ionizing energy loss in silicon for protons, neutrons, pions and electrons. Being very conservative we can state that:

- the non ionizing energy loss of $1GeV$ electrons is ten times lower than the pions loss, regardless of the pion energy.
- the non ionizing energy loss of $1GeV$ electrons is twenty times lower than the neutrons loss, regardless of the neutron energy.

Hence, in order to obtain the same bulk radiation damage, the electron fluence must be ten times the pion fluence and twenty times the neutron fluence. Let us apply this rule to the ALICE case. In order to simplify the calculation we estimate the ALICE pion fluence from the total ionizing dose considering all particles as $m.i.p$.s. This approximation further worsens our test conditions since it maximises the number of particles needed to obtain such dose. Thus, the value of the electron fluence equivalent to the radiation produced in ten years of ALICE operation is:

$$\begin{aligned} \Phi_e &= 10 \cdot \Phi_\pi + 20 \cdot \Phi_n \\ &= 10 \cdot 5 \times 10^{11} + 20 \cdot 3.5 \times 10^{11} \simeq 1 \times 10^{13} e/cm^2 \end{aligned} \tag{1}$$

This fluence corresponds to an absorbed dose in silicon of about $250krad$.
We would like to point out that this dose is more than ten times higher than what is needed to reproduce the ALICE surface damage.

3 Results of the irradiation tests.

The irradiation tests were performed at the LINAC of the "Elettra" Synchrotron in Trieste, where $1GeV$ electrons are produced. We put at the end of the beam pipe a precision x-y movement in which we fixed the board housing the detector. The beam has a gaussian profile with a FMHW of about $2.5\,cm$. In the following subsections we report the results of the measurements performed on the irradiated detectors.

3.1 First irradiation.

The first detector was irradiated as represented in figure 3. The whole drift region facing

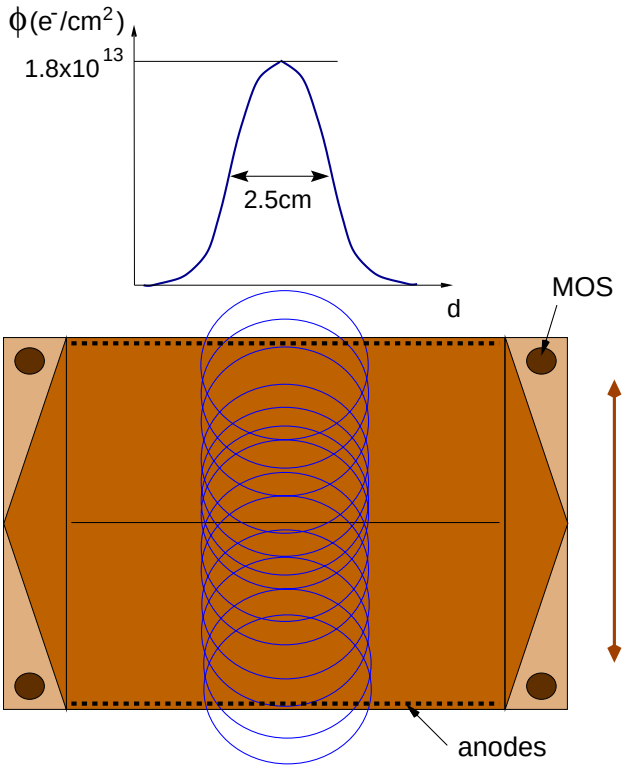

Figure 3: Irradiation test on the first detector.

the central anodes was covered moving the detector up and down. The sample was biased at the nominal operation voltage ($-2400V$) during irradiation. In the region interested by the centre of the beam we reached a peak of the fluence of about $1.8 \times 10^{13} e^{-}/cm^2$ which corresponds to a total ionizing dose of $480krad$. Figure 4a displays the anode current distribution 72 hours after the test. It is clearly visible the gaussian shape of the beam reproduced on the anodic current. In order to appreciate better the irradiation effects, figure 4b presents a comparison of the current before and after the test in logarithmic scale.

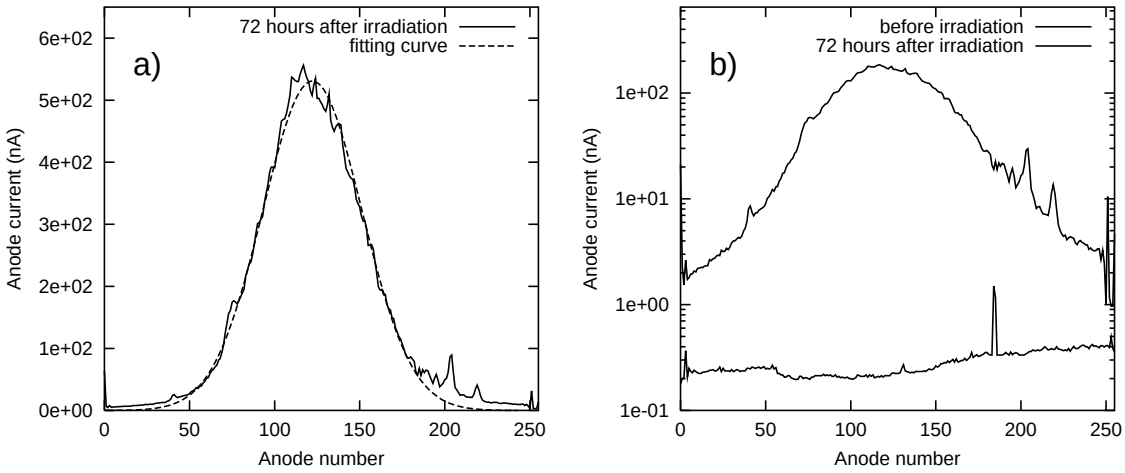

Figure 4: Anode current distribution: a) after irradiation at room temperature, b) before and after irradiation at 20^oC.

Both measurements presented in figure 4b were performed in the climatic chamber at a constant temperature of 20^oC. In this conditions the leakage current is roughly one third of the value at room temperature because we partially remove the heat dissipated by the integrated divider. This controlled environment replicates the ITS one where an air flux will maintain a constant temperature of 20^oC. For this reason, from now on, all the measurements have to be considered at such temperature.

We regularly repeated the measurements of the anode current during 1 month after irradi-

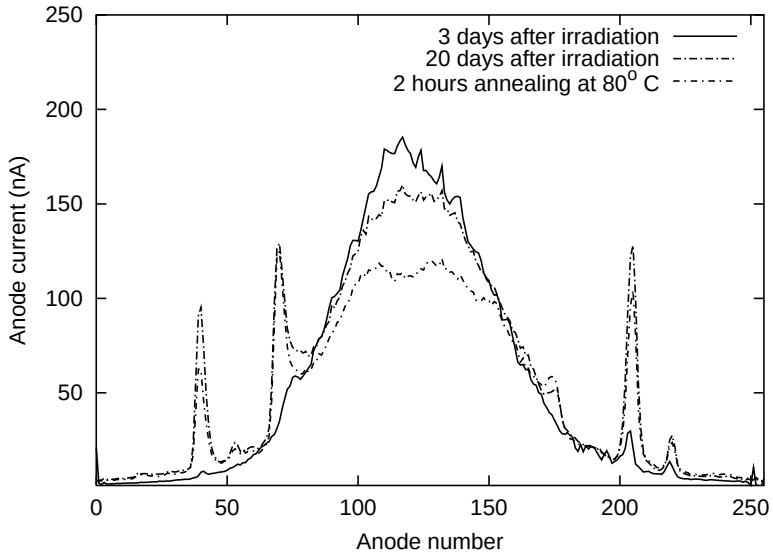

Figure 5: Anode current distribution after different annealing times.

ation. The last tests showed no substantial variations in the distribution, so we decided to

speed up the annealing process heating the detector at 80^oC for 2 hours. Figure 5 presents three distributions respectively after 3 days, 20days, and after the accelerated annealing. It is evident that the annealing effect is more consistent where the silicon was more heavily irradiated. In particular the values around the peak region of the gaussian decrease almost two times, passing from $200nA$ to $100nA$.

It is interesting to note that some peaks are present along the flanks and outside of the gaussian profile. Since these peaks are located also outside the region covered by the beam, it means that the problem is not related to the radiation levels. We found that these hot spots of the current correspond with burned points located along the central cathode which is the most negative one ($-2400V$). Originally we thought that a discharge happened between the box covering the detector and the central cathode. So, in the following tests we tried to minimise that risk, increasing the height of the box and covering the cathode with silicon glue, without obtaining the desired results. Later we understood that the origin of this burned spots is related to the high electron flux emitted by the LINAC. Indeed, the huge ionizing current generated in the detector lowers abruptly the potential of the drift and guard cathodes biased via the integrated divider. On the other hand, the potential of the most negative cathode is forced, within the compliance limits, by the power supply to be fixed at $-2400V$. In this scenario, such cathode is subjected to very high voltages that lead, via breakdown, to it being permanently damaged. Anyway the results of the tests are not corrupted by this problem and provide the desired information.

Exploiting both the non-uniform distribution of the fluence along the beam profile and the segmentation of the anodes, it is possible to reconstruct the dependence between the anode current and the fluence (or dose). Figure 6 displays this relationship for the

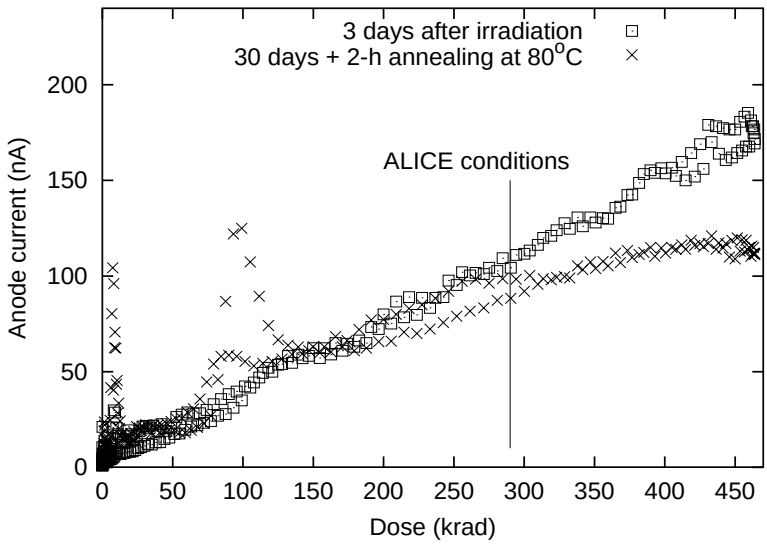

Figure 6: Anode current as a function of the dose for two annealing conditions.

measurements performed 3 days after irradiation and after the annealing in the climatic chamber. We see that in the first case the dependence is perfectly linear while, after the accelerated annealing the current drops for high doses. The peaks visible at low doses are the current hot spots due to the burned points on the central cathode. The vertical line in the plot evidences the electron-equivalent dose expected for ten years of ALICE operation, for which we find an anode current of about $100\,nA$. This value is below the limit imposed by the read-out electronics. After the annealing in the climatic chamber the current is even a little bit lower: about $80\,nA$. Since the detector is expected to absorb that doses during the experiment lifetime, a substantial self-annealing should be taken into account.

3.2 Second irradiation

In the second irradiation test we covered with the beam the whole surface of the detector, as represented in figure 7. The device was moved continuously along horizontal lines

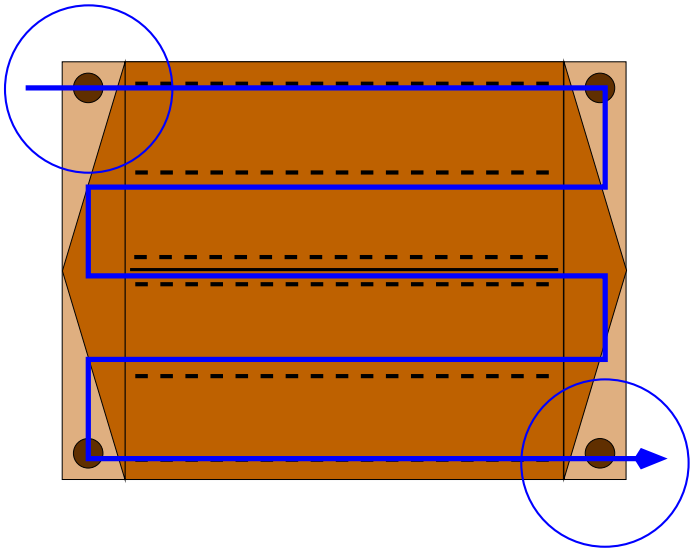

Figure 7: Second irradiation test.

increasing the vertical coordinate by steps of about $0.5mm$. In such a way we obtained a uniform irradiation of the detector. The idea was to irradiate this detector two times, in order to reach first a dose of about $100krad$ a then continue up to $300krad$. However we stopped irradiating at the first step, since the central cathode manifested the problems mentioned in the previous paragraph.

The anode current distribution of both halves is shown in figure 8. We see that the current before irradiation, apart from a small defect, is below $1nA$, while 30 days

after irradiation it is uniformly around $60nA$. Also this detector was put for two hours in the climatic chamber at a temperature of 80^oC in order to accelerate the annealing process, and, as expected, the current changed very slightly. It is important to note that the magnitude of the small defect visible in figure 8a has not increased after the test, indeed, the additional current created by the radiation is simply summed to the original one.

The potential distribution on the integrated voltage divider provides a lot of information as well. In figure 9 the voltage drop every tenth cathode as a function of the cathode number is represented (the central cathode is numbered as 0). In order to have a perfect

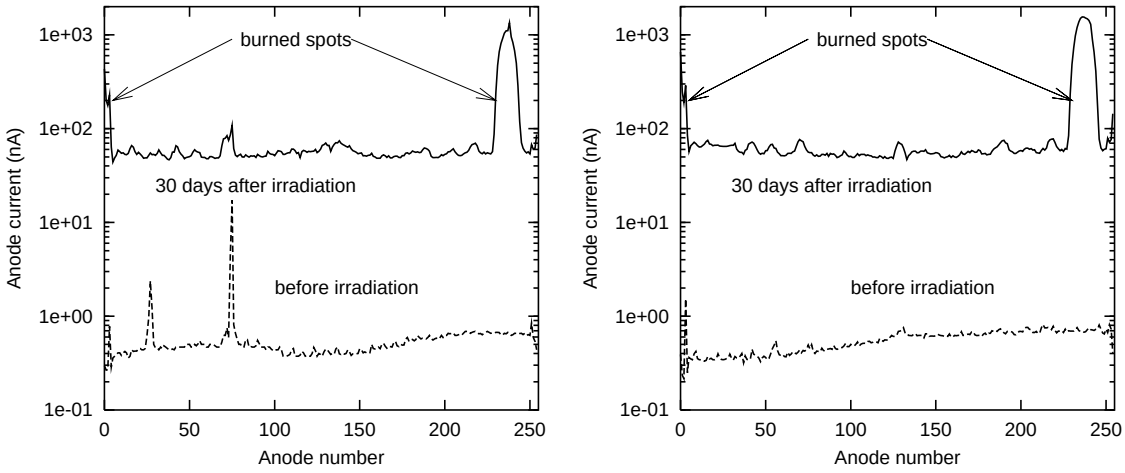

Figure 8: Anode current distribution for the detector irradiated up to $100krad$.

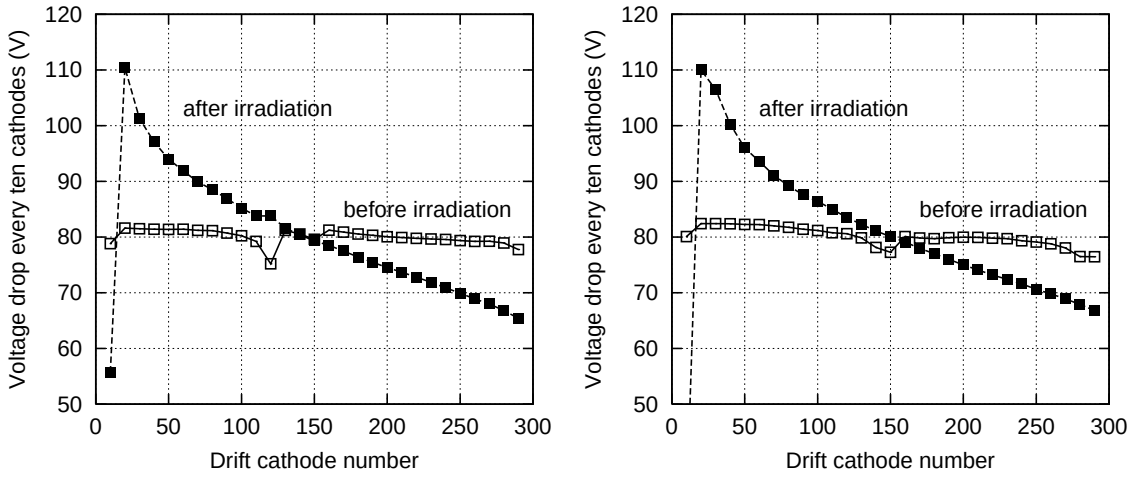

Figure 9: Voltage drop distribution of two integrated dividers of the detector irradiated up to $250krad$.

linear potential distribution along all the drift region we expect a horizontal line at $80V$ (the nominal operation voltage drop is $8\,V$ between consecutive cathodes), and this is verified before irradiation. There is only a small amount of *punch through* [11] which causes a small distortion with respect to a straight line. Instead, after irradiation we note a pronounced slope of the voltage drop distribution. As explained in [9], this is due to the hole component of the leakage current that is collected by the drift cathodes. The high number of holes generated in the bulk are equally shared (if the distribution of generation centres is uniform) among the cathodes and enter the divider chain. Since the holes move toward the more negative potential, the divider current increases gradually from one cathode to cathode increasing, as a consequence, the voltage drop on the resistors chain. Moreover, since the bias voltage is fixed, a straight line with a certain slope has to cross $80V$ exactly at the cathode number 150. As far as our detector is concerned, we see that beyond the cathode number 100 the curve is a perfect straight line which slope is proportional to the leakage current and consequently to the dose given to the detector. Below the cathode 100 we start gradually to "see" the burnings on the cathode number 0 and the curves start to deviate from the straight line. It should be noted that this measurement was performed at room temperature, thus, cooling the detector at 20^oC in the climatic chamber, the slope is three times less steeper as soon as the leakage current is three times lower. Finally, we note that the small distortions due to the *punch through* current are disappeared after irradiation. This is linked to the growth of the oxide charge which makes more effective the operation of the field-plates [11].

3.3 Third irradiation

The third detector was irradiated uniformly on the whole area as the previous one. Along with the detector, we irradiated also a diode taken from the same wafer. We put the diode just in front of the detector in order to irradiate both devices in the same way. The absorbed dose in silicon was $250krad$ which is about the electron-equivalent dose expected for ALICE, as far as the bulk damage is concerned.

Figure 10 shows the anode current distributions respectively before irradiation and 15 days plus an annealing time of two hours at 80^oC after irradiation. From the first plot we see that the mean level of the anode current is about $70nA$; before the accelerated annealing it was about $100nA$. Both values are in good agreement with the graph shown in figure 6. For the second half-detector (right plot of figure 10), the mean value is smaller than the other because the x-y movement stopped three y-steps before the end of irradiation. Also in this detector some peaks appeared after the test (central anodes) due to the damage of the central cathode.

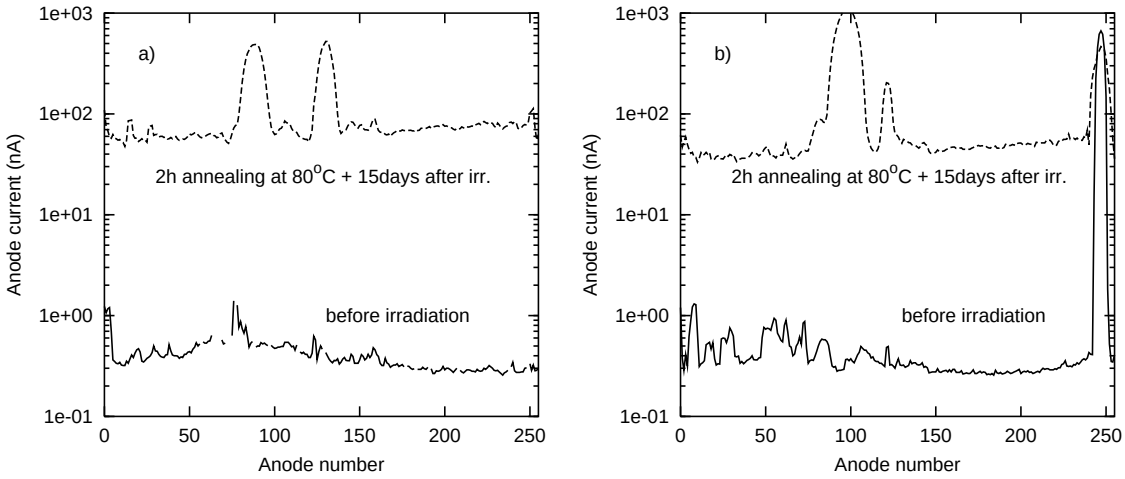

Figure 10: Current distribution of both array of anodes of the detector irradiated with $250krad$.

Looking at the potential distribution on the integrated dividers we see that on one detector's side (figure 11a) the irradiation caused, as expected, a growth of the slope of the line representing the voltage drops on the resistor chain. On the other side (figure 11b), besides the steep slope, we note the presence of two steps. One is already present before

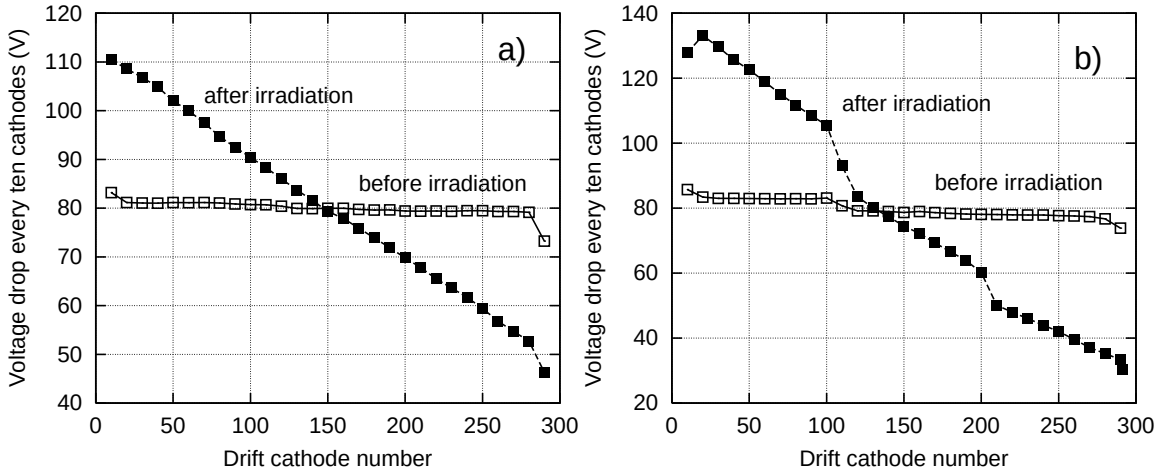

Figure 11: Potential distribution of two integrated dividers, one per side, of the detector irradiated with $250krad$.

irradiation and it is related to the current peak visible at the far left of the figure 10b. It is worth noting that, as in the previous detector, the peak magnitude did not change after irradiation. The second step, around the cathode number 200, was also present before irradiation in the very first measurement we performed on the detector, and then

disappeared after the burn-in time. Very likely the manifestation of this defect depends on the electric field due to the positive fixed oxide charge that, after the burn-in time, is partially compensated by the environmental humidity. After irradiation, the oxide charge increases abruptly (see following discussion) and clearly reactivates the defect. Since a defect generating high current in the drift region has to be seen both as a step in the voltage drop distribution and as an anodic current peak [9], one of the central peaks in figure 10 should be related to such voltage step. Otherwise the problem could be situated in the guard region; in that case the electron component of the leakage current is collected by the n-ring.

As far as the fixed oxide charge is concerned, the four on-board MOS capacitors allow its monitoring. The high frequency $C - V$ measurements, both before and after irradiation, are presented in figure 12. Before irradiation the flat band voltage is $2V$

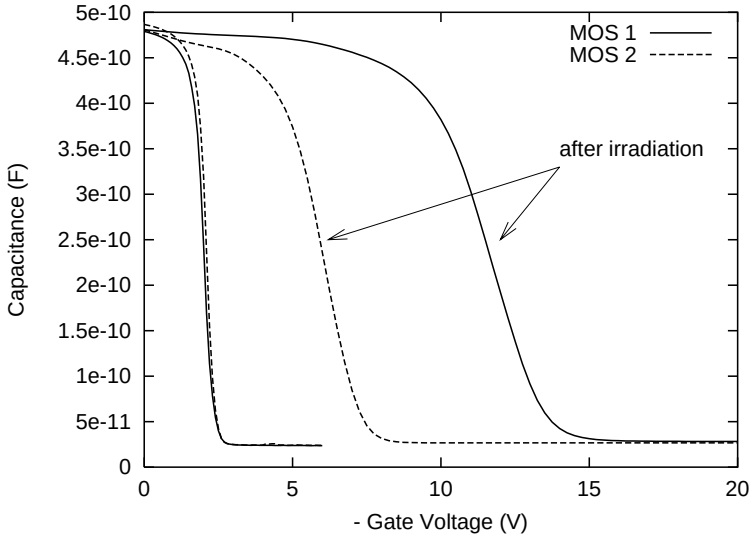

Figure 12: High frequency C-V measurements for two on-board MOS capacitors respectively before and after irradiation..

providing an oxide charge density slightly above $1 \times 10^{11} q/cm^2$. As mentioned before, the motors holding the detector stopped three y-steps before the end of the irradiation. Since the MOS are placed at the corners of the detector (figure 1) they underwent to different fluences, and this explains the strong discrepancy of the $C - V$ measurement after irradiation. MOS1, which absorbed all the dose ($250krad$) presents an oxide charge density of $9.5 \times 10^{11} q/cm^2$.

As above-mentioned, along with the detector we irradiated also a diode. The $C-V$ measurement is substantially unchanged after irradiation. On the other hand, the $I - V$ measurement showed a full depletion leakage current 600 times higher than the original.

From this measurement we can obtain the current damage coefficient, defined as:

$$\alpha = \frac{\Delta I}{\Phi V} \tag{2}$$

where ΔI is the difference of the leakage current after and before the irradiation, Φ is the particle fluence, and V the depleted volume. This parameter gives an idea of the bulk damage created by a particle having a certain energy.In our case, one month after irradiation, it is about $2.5 \times 10^{-18} A/cm$. Comparing this value with the current damage coefficient of pions ($\sim 2.8 \times 10^{-17} A/cm$ [12]) and neutrons ($\sim 4 \times 10^{-17} A/cm$ [13]) we find that our estimation of the electron fluence has been carried out correctly.

In order to verify the performance of the MOS injectors after irradiation, the detector was bonded to integrated preamplifier/line driver electronics specially designed for silicon drift detectors [4]. Figure 13 shows the amplitude of the anode signal as a function of the anode number, when applying to the central injector line a negative pulse with an amplitude of $3V$, a width of $50ns$ and a frequency of $100Hz$. From this plot one can see the periodicity of the point-like MOS injectors: 1 every 8 anodes.

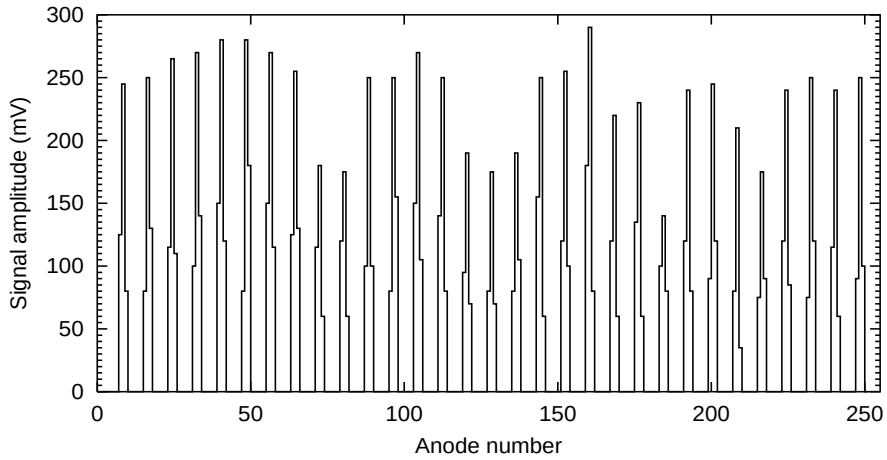

Figure 13: Signal clusters corresponding to the charge injected by the central injector line.

The behaviour of the injectors results strongly improved with the irradiation. Firstly, with a pulse amplitude of $3 - 4V$ we obtain the needed signal at the anodes, because a great amount of electrons are attracted under the oxide by the high positive oxide charge density. Dealing with MOS injectors, one should guarantee a certain level of the oxide charge density in order to have a sufficient signal amplitude at the anodes. For example, the injectors of this detector were scarcely visible before irradiation. The plot in figure 14 shows the amplitude of the anode signal as a function of the pulse amplitude for this detector after irradiation, and for a non-irradiated detector (from [4]). The anode

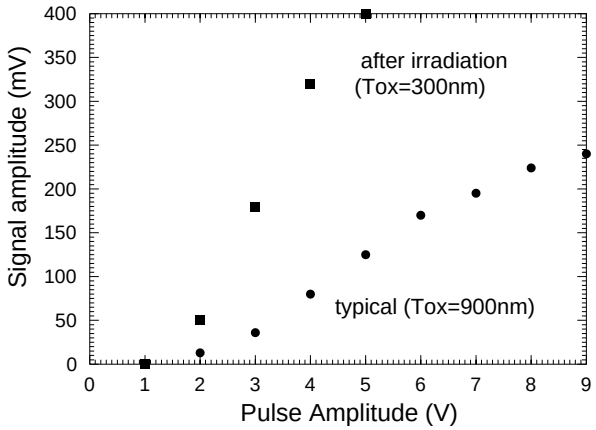

Figure 14: Amplitude of the anode signal as a function of the pulse amplitude for the irradiated detector and for a non-irradiated detector having an oxide thickness three times higher.

signal amplitude of the irradiated detector is three times higher than the other because the oxide thickness of the MOS injector is three times smaller. It is important to note that the characteristic of the non-irradiated detector starts to saturate at some $200mV$ because with one pulse we empty the potential pocket of electrons. Instead, the irradiated one starts to saturate at $350mV$ just because of the limited dynamic range of the electronics. A second characteristic strongly improved after irradiation, is the maximum repeat rate of the injectors, as represented in figure 15. The limitation of the pulse frequency is due to

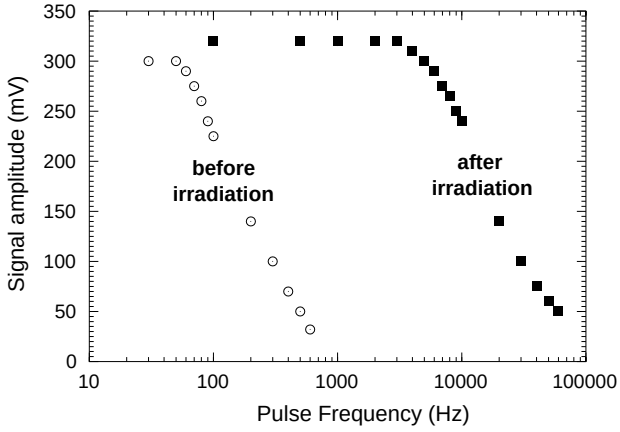

Figure 15: Semilogarithmic plot of the signal amplitude as a function of the frequency of the injection pulse.

the refill velocity of the potential pocket below the gate when it is emptied of electrons applying a negative pulse. The increased surface generation caused by the radiation greatly

increases the frequency cut-off.

4 Conclusions.

Irradiation tests using $1GeV$ electrons demonstrate that the ALICE-D2 silicon drift detector design is sufficiently radiation resistant for the full operational lifetime of the ALICE experiment. The anode leakage current expected after ten years of operation is below the limits imposed by requirements of the read-out electronics. As expected, the linearity of the integrated potential divider is degraded by the increase in leakage current, but in such a way that the on-board MOS injectors should be sufficient to allow on-line monitoring and correction of this degradation. Finally, the performance of the MOS injectors actually improves after irradiation - again in line with expectations.

5 Acknowledgements

We would like to thank Andrea Vacchi for the constant encouragement and support, Luciano Bosisio for the useful discussions and Irina Rachevskaia for helping us in the measurements.

References

[1] Inner Tracking System, ALICE Technical Design Report, CERN/LHCC, June 1999.

[2] V. Bonvicini *et al.*, Nucl. Instr. and Meth. **A439** (2000) 476.

[3] D. Nouais *et al.*, Nucl. Phys. B (Proc. Suppl.) **78** (1999) 252-258.

[4] V. Bonvicini *et al.*, Il Nuovo Cimento, Vol. **112A** N. 1-2, January-February 1999, 137-146.

[5] A. Rashevsky *et al.*, Nucl. Instr. and Meth. **A461** (2001) 133-138.

[6] G. Lutz, "*Semiconductor radiation detectors*", Springer, 1999.

[7] T. R Oldham, "*Ionizing radiation effects in MOS oxides*", World Scientific, 1999.

[8] P. Giubellino *et al.*, ALICE-INT-2001-03, January 2001.

[9] C. Piemonte, A. Rashevsky, D. Nouais, INFN/TC-00/04, 2000.

[10] G.P. Summers *et al.*, IEEE NS Vol.**40** N. 6, December 1993, 1372.

[11] C. Piemonte, A. Rashevsky, INFN/TC-02/08, 10 aprile 2002.

[12] S.J. Bates *et al.*, CERN-ECP/95-26, November 1995.

[13] A. Ruzin *et al.*, IEEE NS Vol. **46** N.5, October 1999, 1310.